Atomic Energy of Canada Limited

CANDU-BLW EXPERIMENTS IN ZED-2

PART I: REFUELLING EXPERIMENT

by

R. E. KAY and C. J. TANNER

Chalk River, Ontario

January 1967

AECL-2667

CANDU-BLW EXPERIMENTS IN ZED-2

PART I: REFUELLING EXPERIMENT

by

R.E. Kay and C.J. Tanner

A B S T R A C T

Experiments have been performed in a simulated CANDU-BLW lattice in ZED-2 to determine the reactivity effect and the perturbing effect on the surrounding lattice of replacing the fuel in the central cell of the lattice by light water. This procedure simulates two stages in the refuelling sequence of the proposed CANDU-BLW reactor.

The maximum neutron density perturbation observed in surrounding fuel assemblies was a depression $\sim$ 16% at the assemblies immediately adjacent to the perturbation.

Chalk River, Ontario
January 1967

AECL-2667

TABLE OF CONTENTS

FIGURES

TABLES

I. INTRODUCTION

This report is the first of a series describing experiments performed in the heavy-water-moderated critical facility ZED-2[1] to investigate specific problems relating to the proposed CANDU-BLW reactor[2].

During the proposed on-load refuelling of the BLW reactor all the fuel will be removed from one reactor channel, causing the channel to fill with light water coolant. The experiments described here investigate the reactivity effects and flux perturbation effects on the surrounding lattice, of a similar operation performed in a mock-up lattice in ZED-2.

II. FUEL AND LATTICE

Because prototype BLW fuel was not available the experiments were performed using a mock-up lattice which approximated in fuel, coolant and moderator absorption areas to that proposed for the prototype BLW reactor. This mock-up lattice was composed of 53, 28-rod UO_2 fuel assemblies arranged in ZED-2 in a square lattice of spacing 27.94 cm (11 in.). Details of the 28-rod UO_2 fuel assemblies are given in Figure 1. Each fuel rod consists of natural uranium oxide fuel pellets (1.42 cm dia., density 10.45 g/cm^3) contained in Zircaloy -2 sheaths (1.43 I.D., 0.045 cm wall). Four, eight and sixteen of these rods are located by end plates on three circles of radii 2.326 cm, 5.304 cm and 8.412 cm respectively to form a fuel bundle. A fuel assembly consists of five of these bundles within aluminum pressure (I.D. 10.19 cm, O.D. 10.78 cm) and calandria (I.D. 12.46 cm, O.D. 12.74 cm) tubes.

During operation the coolant in the BLW reactor will be a mixture of boiling light water and up to 33% steam; in the experiments described here the coolant was room temperature light water.

A comparison of the absorption areas of a lattice cell of the ZED-2 mock-up and a proposed BLW lattice[3] is made in Table I.

The mock-up lattice has a very low reactivity and to achieve a critical system in ZED-2 a 'driver' region was required; Figure 2 illustrates the arrangement used. The simulated BLW region was surrounded by an annulus of 120 ZEEP 3.257 cm (1.282 in.) diameter natural uranium metal fuel rods in a square lattice of pitch 13.97 cm (5½ in.) [close to the pitch for maximum buckling]. Between the BLW zone and the driver zone was a 'buffer' zone of twenty air cooled 7-rod natural uranium oxide fuel assemblies.

FIG. 1 CROSS SECTION THROUGH 28 ROD FUEL ASSEMBLY

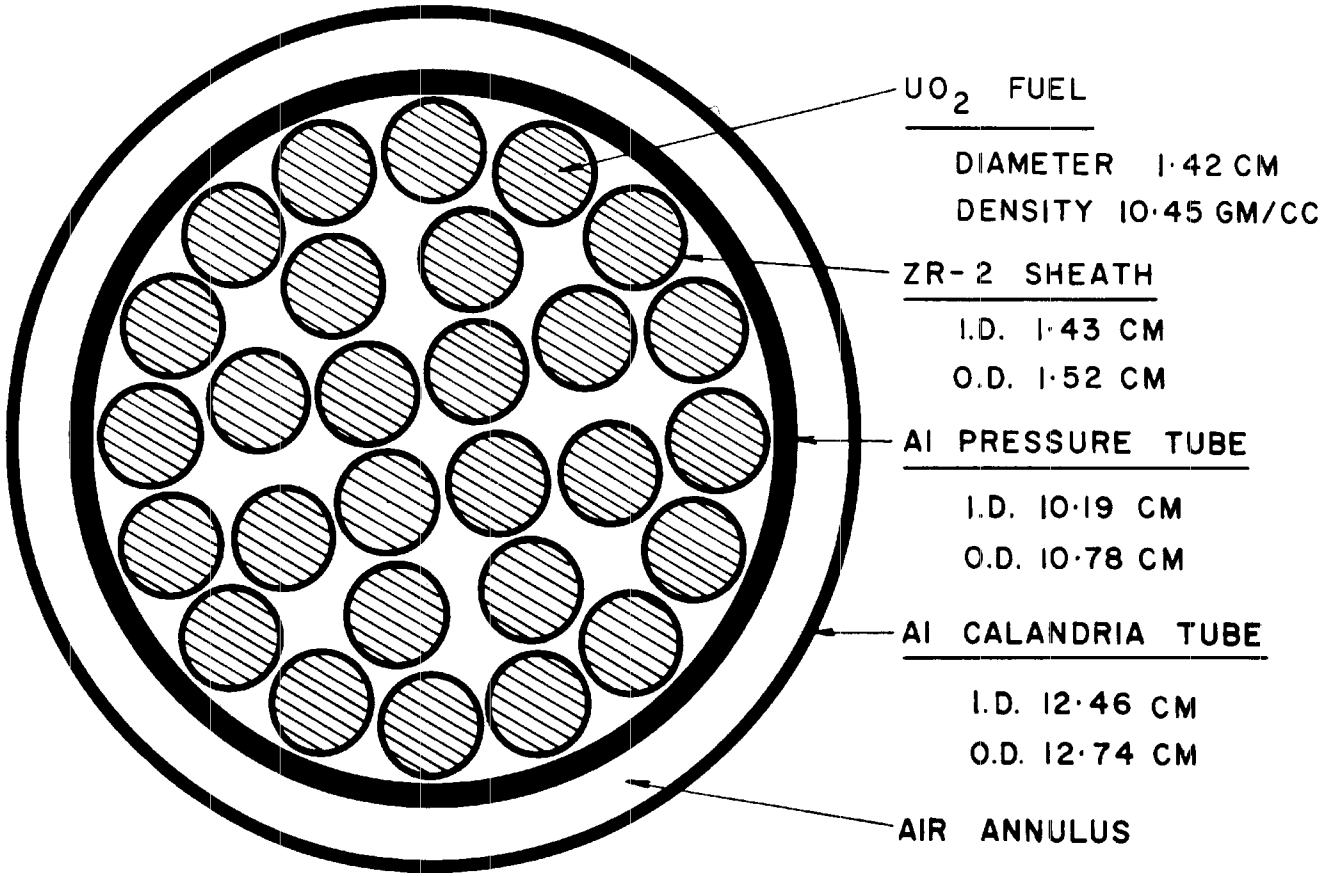

TABLE 1: COMPARISON OF PROPOSED BLW LATTICE CELL AND ZED-2 MOCK-UP LATTICE CELL

Cell Region	BLW (Case 1001-40)			ZED-2 Mock-up		
	Material	Area (cm^2)	Area x Σ_a (cm^2/cm)	Material	Area[a] (cm^2)	Area x Σ_a (cm^2/cm)
Fuel	UO_2	45.88	7.80	UO_2	44.41	7.55
Sheath	Zr-2	8.42	0.08	Zr-2	5.90	0.05
Coolant	H_2O[b]	26.60	0.59	H_2O[b]	30.67	0.67
Pressure Tube	Zr/Nb	8.02	0.07	Al	9.75	0.15
Calandria Tube	Zr-2	3.70	0.03	Al	5.50	0.08
Moderator	D_2O	671.84	0.07	D_2O	653.16	0.07
Total absorption Area			8.64			8.57

a) Cross sectional areas for a plane through mid length of fuel bundle.

b) H_2O density assumed = 1.0 g/cm^3.

FIG. 2 B.L.W. (AS.) LATTICE ARRANGEMENT IN ZED-2

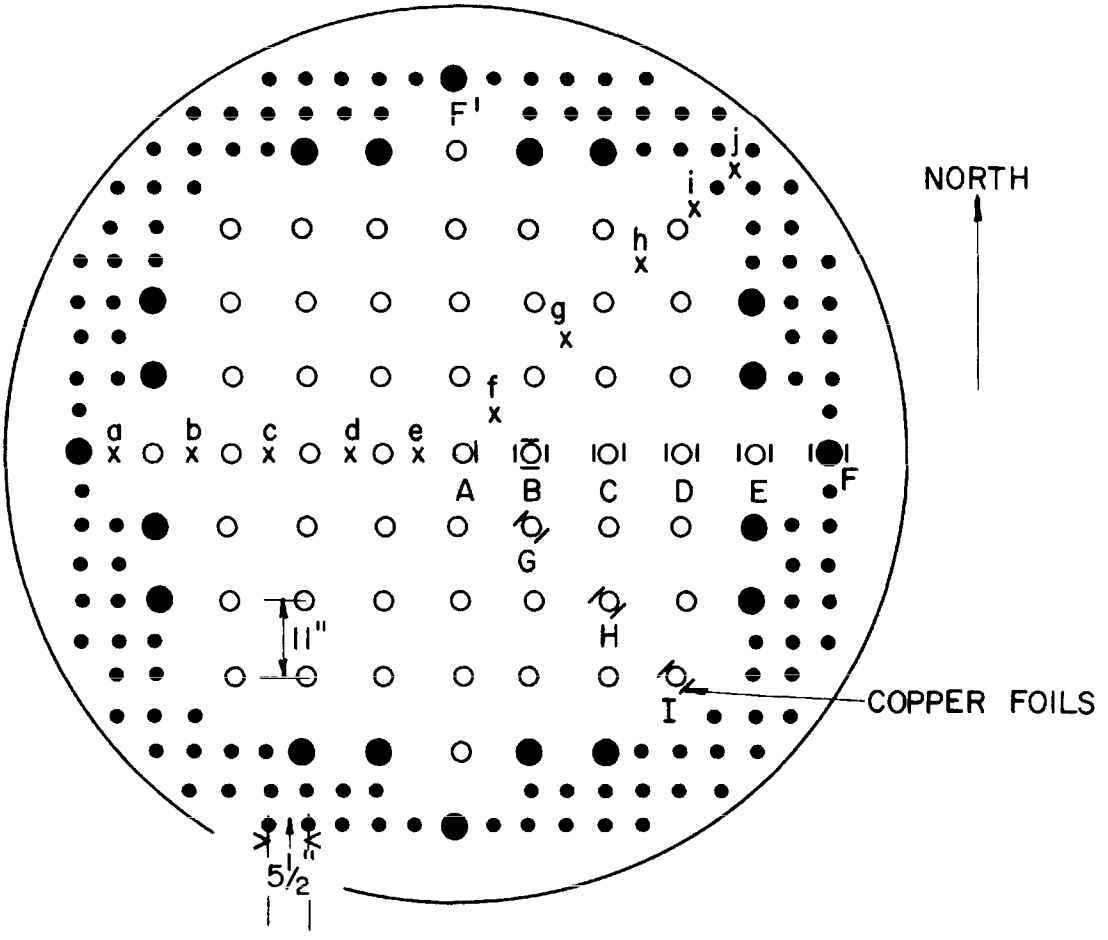

O 28 ROD UO_2 FUEL

● 7 ROD UO_2 FUEL

• ZEEP FUEL ROD

x FOIL THIMBLE

This buffer zone helped match the spectrum differences at the driver-BLW zone interface. Details of the ZEEP and 7-rod UO_2 fuel assemblies are given in references 4 and 5.

III. EXPERIMENTS

1. Macroscopic Flux Perturbation Measurements

Experiments were performed to compare the neutron density distributions at typical lattice positions when no perturbations were present and when the fuel in the assembly at the centre of the lattice (assembly A, Fig. 2) was replaced by light water, these two conditions approximating two of the stages in the refuelling sequence of the proposed BLW reactor. Since the change made was essentially uniformly distributed axially over the full core height only radial effects were investigated.

Figure 2 represents both the perturbed and unperturbed lattices; 'a' through 'j' are thin walled aluminum thimbles located at cell boundary positions holding 1.13 cm (0.444 in.) dia., 0.025 cm (0.010 in.) thick copper foils. Foils were mounted in all thimbles at heights of 135 cm (near the point of maximum axial flux) and 185 cm. [All heights are given relative to the floor of the reactor vessel.] In addition, thimble 'a' carried a full vertical set of copper foils located at 10 cm intervals from 15 cm to 235 cm. To investigate the perturbations produced at neighbouring fuel assemblies similar copper foils were taped to the outside of the calandria tube of assemblies B to F, in the positions indicated in Figure 2 and on the Northwest and Southeast sides of assemblies G to I, at elevations of 135 cm and 185 cm. (Fuel assembly F' was used in preference to assembly F for ease of foil loading; both positions are equivalent.) In the unperturbed lattice foils were placed on the East side, and in the perturbed

lattice on the North, South and East sides of the calandria tube of assembly A.

In addition thimbles 'e' and 'j' of the unperturbed lattice also carried full vertical sets of copper foils. This enabled the core axial buckling to be investigated at three core radii [see Appendix A].

2. Detailed Neutron Density Measurements in Central Cell of Perturbed Lattice

The copper foil activities allowed determination of the pile macroscopic perturbations. The detailed neutron density distributions in the central cell containing the perturbation were investigated by manganese wire activations; these could be compared with previously measured neutron densities in an unperturbed cell.(6)

Figure 3 illustrates a lucite cruciform suspended within the light water filled assembly with arms aligned North-South and East-West and Figure 4 diagramatically illustrates both this cruciform and an aluminum framework, taped to the calandria tube of assembly A having arms extending East and Southeast into the moderator. Both the cruciform and the aluminum framework were located at an elevation of 135 cm and held 0.51 mm diameter, 5 mm long Mn-10% Ni wires in positions indicated in Figure 4.

3. Neutron Spectrum Measurements

To compare the perturbed and unperturbed distributions accurately it was necessary to correct the measured foil and wire relative activities for epithermal neutron activation to give relative total neutron densities. In previous experiments $r\sqrt{T_n/T_o}$ values had been measured at several cell boundary positions

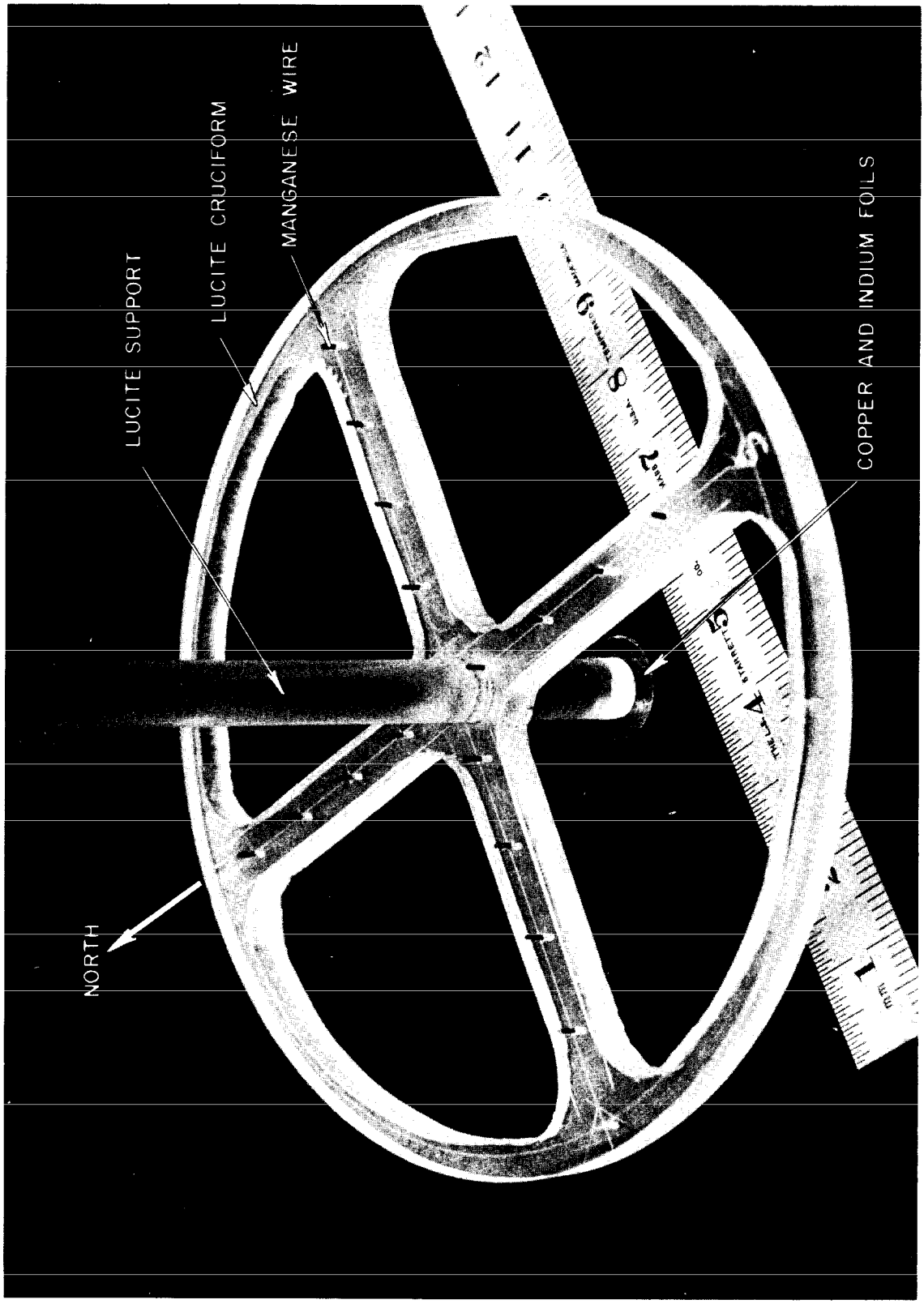

FIG. 3 FOIL AND WIRE SUSPENSION IN LIGHT WATER

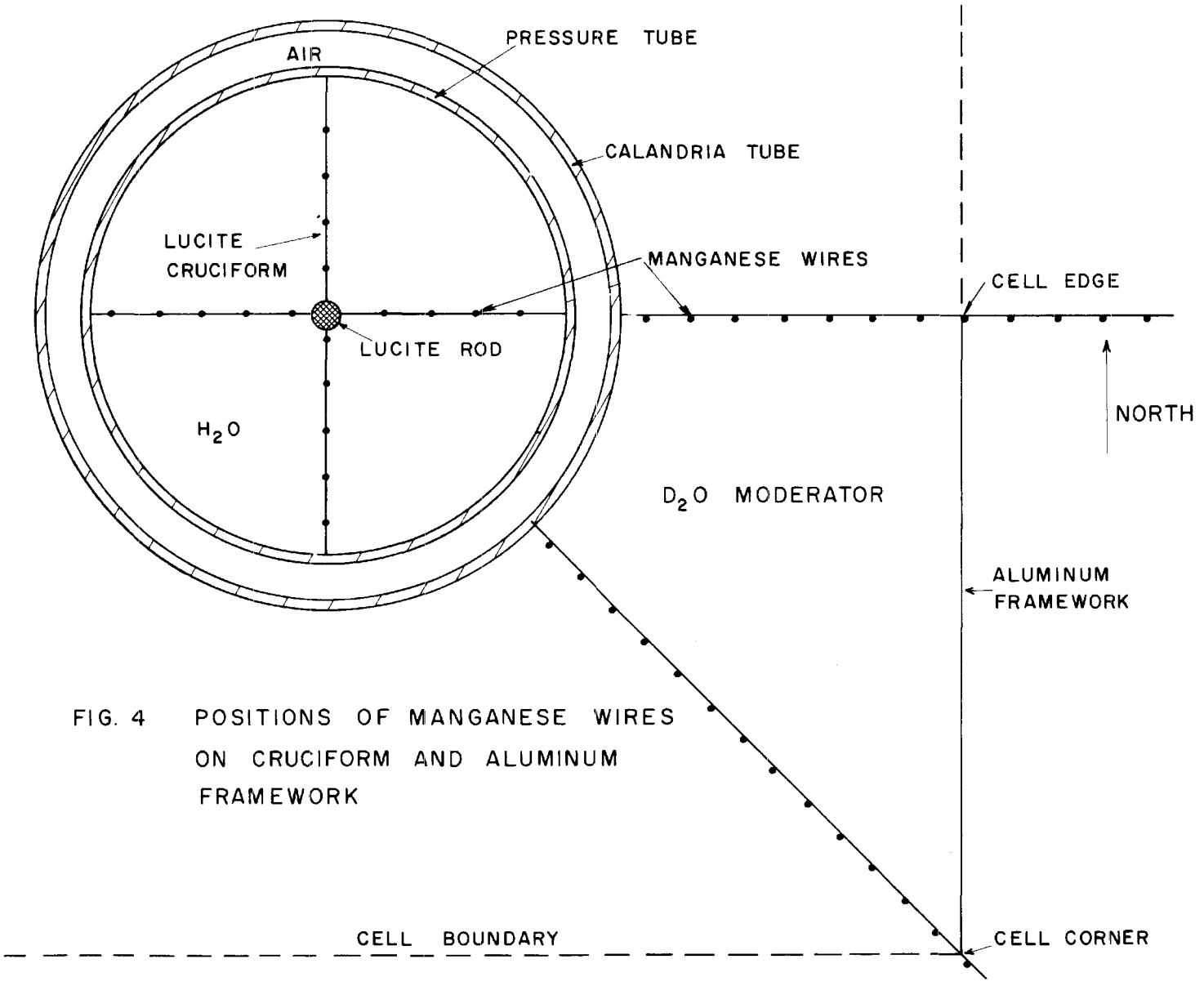

FIG. 4 POSITIONS OF MANGANESE WIRES ON CRUCIFORM AND ALUMINUM FRAMEWORK

throughout the unperturbed core by the cadmium-ratio method[7] using thin indium foils.

In the perturbed lattice, $r\sqrt{T_n/T_o}$ measurements were made at the centre of the water filled tube (see Fig. 3), on the surface of the calandria tube of assembly A, on the West side of the calandria tube of assembly B and at the cell edge of the central cell, using pairs of copper and indium foils and normalizing their relative activities to a similar pair of foils in thimble 'b' where $r\sqrt{T_n/T_o}$ was known from a cadmium-ratio measurement made using thin indium foils.

4. Copper-Manganese Normalization

Normalization of the copper foil and manganese wire relative neutron densities in the perturbed lattice was made by comparison of the relative total neutron densities obtained from copper foils and manganese wires placed together on the aluminum framework at the edge and corner of the central cell (see Fig. 4) and at elevations of 125 cm and 145 cm in thimble 'b'.

5. Reactivity Measurements

Pile critical heights were determined for the following conditions:

a) Unperturbed lattice
b) Fuel in central assembly replaced by H_2O
c) Fuel and coolant in central assembly replaced by air
d) Fuel and coolant in central assembly replaced by D_2O
e) The unperturbed lattice with a 2.54 mm diameter cobalt wire located in the central cell.

A lead weight used to counteract the buoyancy of the D_2O moderator was attached to the bottom of the central assembly and was present in all experiments (its measured effect on the pile

critical heights was ~ 0.070 cm). [Although experiments c) and d) are not directly related to the refuelling problem they give additional information for normalization of computer codes.]

Experiment e) was performed with a full length cobalt wire extending through the moderator at the cell edge position of the central cell. Knowing the flux depression factor for this wire its reactivity effect can be calculated and related to the change in critical height required to keep the reactor critical, hence providing a calibration factor to relate other critical height changes to reactivity changes.

IV. RESULTS AND DISCUSSION

1. Macroscopic Perturbations

Relative copper foil activities A(r,z) were converted to relative total neutron densities n(r,z) using the expression

$$n(r,z) = A(r,z) \Big/ \left(G_{th} g + G_r s_o \, r\sqrt{T_n/T_o} \right) \quad \ldots\ldots\ldots 1)$$

where G_{th}, g, G_r and s_o have their usual meanings in the Westcott notation.[8]

For the unperturbed lattice the previously measured $r\sqrt{T_n/T_o}$ values were used. At locations 'y' within the unperturbed cell where $r\sqrt{T_n/T_o}$ was not measured it was assumed that

$$\left[r\sqrt{T_n/T_o} \right]_y = \left[r\sqrt{T_n/T_o} \right]_p \cdot \frac{A_p}{A_y}$$

where p is a location within the cell where $r\sqrt{T_n/T_o}$ was measured and A are copper foil activities. This interpolation within a cell

from points at which measurements were made introduces negligible error since copper has a low resonance integral and the epithermal activation was < 1% of the thermal activation at all points.

For the perturbed lattice, the $r\sqrt{T_n/T_o}$ values were assumed to be the same as in the unperturbed lattice except in the region immediately surrounding the perturbation, where the measured values of $r\sqrt{T_n/T_o}$ were used (see Table 2 and Sec. V-2)

The resulting relative total neutron densities in the unperturbed and perturbed lattices normalized to 1.000 at thimble 'a' at an elevation of 135 cm are given in Tables 3 and 4.

Figure 5 illustrates the relative total neutron density distributions along the West and Northeast radii of the unperturbed and perturbed cores [in all figures curves are drawn by eye]. Note the azimuthal variation of the distributions at radii > 90 cm due to the arrangement at the lattice. The radial distributions follow an I_o function at radii < ~ 90 cm; this is a result of the low reactivity of the simulated BLW region which results in a net incurrent of neutrons from the ZEEP driver region. When the perturbation is introduced the overall neutron density distribution in the core is depressed, the depression extending out to radii ~ 115 cm.

The relative neutron densities at calandria tube positions in the perturbed and unperturbed lattices are given in Fig. 6 which illustrates a peaking in the neutron density distributions in the locality of the perturbation superimposed upon the general depression across the core.

To compare quantitatively the perturbed and unperturbed neutron density distributions, it is necessary to normalize the two experiments to a single point and make an allowance for the

TABLE 2: $r\sqrt{T_n/T_o}$ VALUES IN PERTURBED LATTICE

Location	$r\sqrt{T_n/T_o}$	$r\sqrt{T_n/T_o} \times n'$ Perturbed
Thimble 'b'	0.0207 [a]	
A(N)	0.0084 [b]	0.007
B(W)	0.0209 [b]	0.014
Cell Edge	0.0130 [b]	0.011
Centre of H_2O	0.0038 [b]	0.002
Thimble 'e' (unperturbed)	0.0216 [a]	0.022 [c]

a) Indium-Cadmium Ratio Measurement.

b) Cu-In Activity Ratio Measurement Relative to [a].

c) $\left[r\sqrt{T_n/T_o} \times n'\right]$ thimble 'e' unperturbed

TABLE 3: NORMALIZED RELATIVE TOTAL NEUTRON DENSITY DISTRIBUTION — REFERENCE LATTICE

Location	Elevation Above Floor of Calandria (cm)																						
	15	25	35	45	55	65	75	85	95	105	115	125	135	145	155	165	175	185	195	205	215	225	235
a	0.404	0.479	0.570	0.666	0.753	0.829	0.893	0.945	0.984	1.009	1.020	1.017	1.000	0.968	0.923	0.866	0.796	0.715	0.624	0.524	0.419	0.300	0.172
b													1.094					0.779					
c													1.052					0.750					
d													1.027					0.730					
e	0.388	0.475	0.581	0.683	0.772	0.850	0.916	0.970	1.009	1.035	1.046	1.043	1.024	0.992	0.945	0.886	0.814	0.730	0.636	0.534	0.430	0.308	0.180
f													1.110					0.777					
g													1.130					0.801					
h													1.161					0.831					
i													0.889					0.640					
j	0.328	0.365	0.428	0.493	0.554	0.608	0.653	0.689	0.716	0.734	0.741	0.738	0.725	0.703	0.670	0.629	0.579	0.521	0.456	0.385	0.307	0.225	0.134
A(E)													0.779					0.554					
B(N)													0.804					0.570					
B(S)													0.777					0.556					
B(E)													0.775					0.557					
B(W)													0.786					0.562					
C(E)													0.804					0.570					
C(W)													0.785					0.570					
D(E)													0.838					0.619					
D(W)													0.814					0.606					
E(E)													0.782					0.565					
E(W)													0.850					0.594					
F(E)													0.510					0.382					
F(W)													0.491					0.359					
G(NW)													0.791					0.568					
G(SE)													0.794					0.568					
H(NW)													0.806					0.566					
H(SE)													0.807					0.584					
I(NW)													0.833					0.580					
I(SE)													0.755					0.554					

TABLE 4: NORMALIZED RELATIVE TOTAL NEUTRON DENSITY DISTRIBUTION — PERTURBED LATTICE

Location	Elevation Above Floor of Calandria (cm)																						
	15	25	35	45	55	65	75	85	95	105	115	125	135	145	155	165	175	185	195	205	215	225	235
a	0.381	0.459	0.547	0.641	0.725	0.799	0.863	0.917	0.958	0.988	1.004	1.008	1.000	0.978	0.944	0.898	0.840	0.772	0.694	0.607	0.513	0.409	0.298
b													1.067					0.831					
c													0.997					0.772					
d													0.904					0.695					
e													0.853					0.656					
f													0.908					0.697					
g													1.039					0.807					
h													1.143					0.880					
i													0.894					0.690					
j													0.733					0.566					
A(N)													0.809										
A(S)													0.804										
A(E)																		0.625					
B(N)													0.673					0.523					
B(S)													0.654					0.506					
B(E)													0.673					0.521					
B(W)													0.646					0.501					
C(E)													0.759					0.582					
C(W)													0.711					0.555					
D(E)													0.815					0.647					
D(W)													0.777					0.616					
E(E)													0.781					0.604					
E(W)													0.835					0.631					
F(E)													0.492					0.395					
F(W)													0.505					0.402					
G(NW)													0.671					0.524					
G(SE)													0.719					0.552					
H(NW)													0.765					0.585					
H(SE)													0.789					0.611					
I(NW)													0.828					0.618					
I(SE)													0.760					0.599					

FIG. 5 RADIAL NEUTRON DENSITY DISTRIBUTIONS IN PERTURBED AND UNPERTURBED LATTICE: FOILS IN THIMBLES AT CELL BOUNDARIES, ELEVATION 135 cm

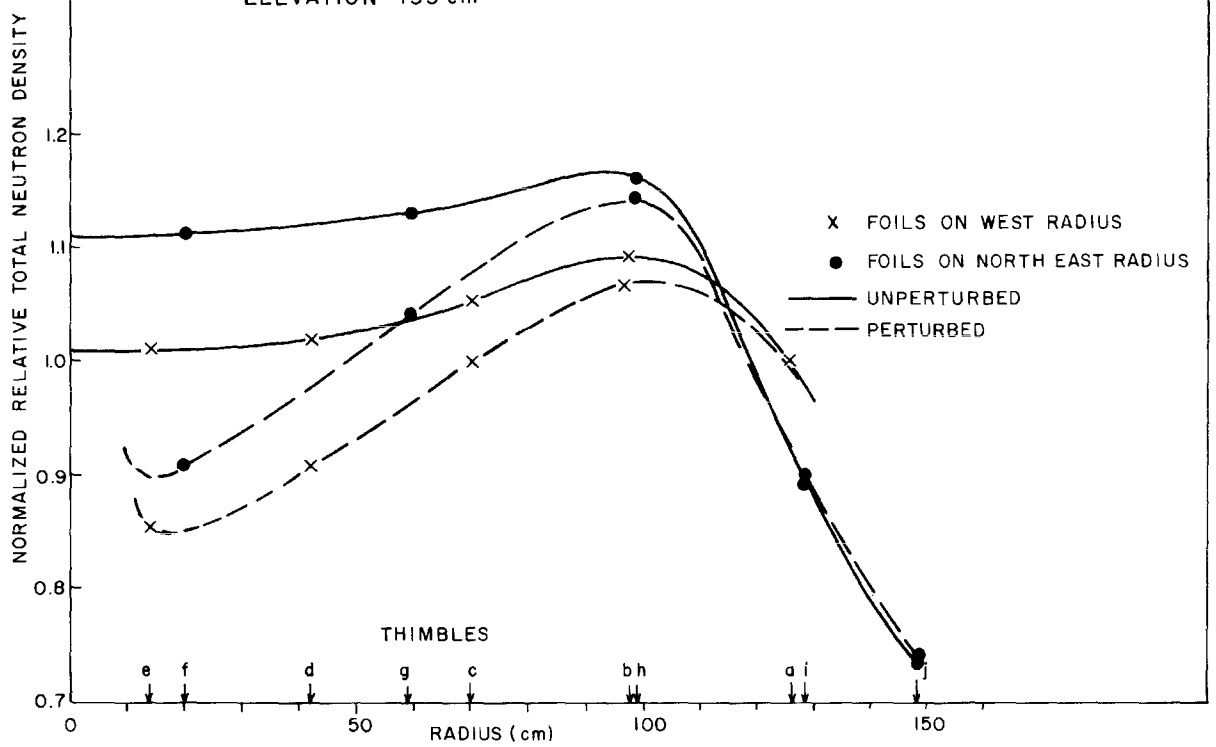

FIG. 6 RADIAL NEUTRON DENSITY DISTRIBUTIONS IN PERTURBED AND UNPERTURBED LATTICE: FOILS ON CALANDRIA TUBES, ELEVATION 135 cm

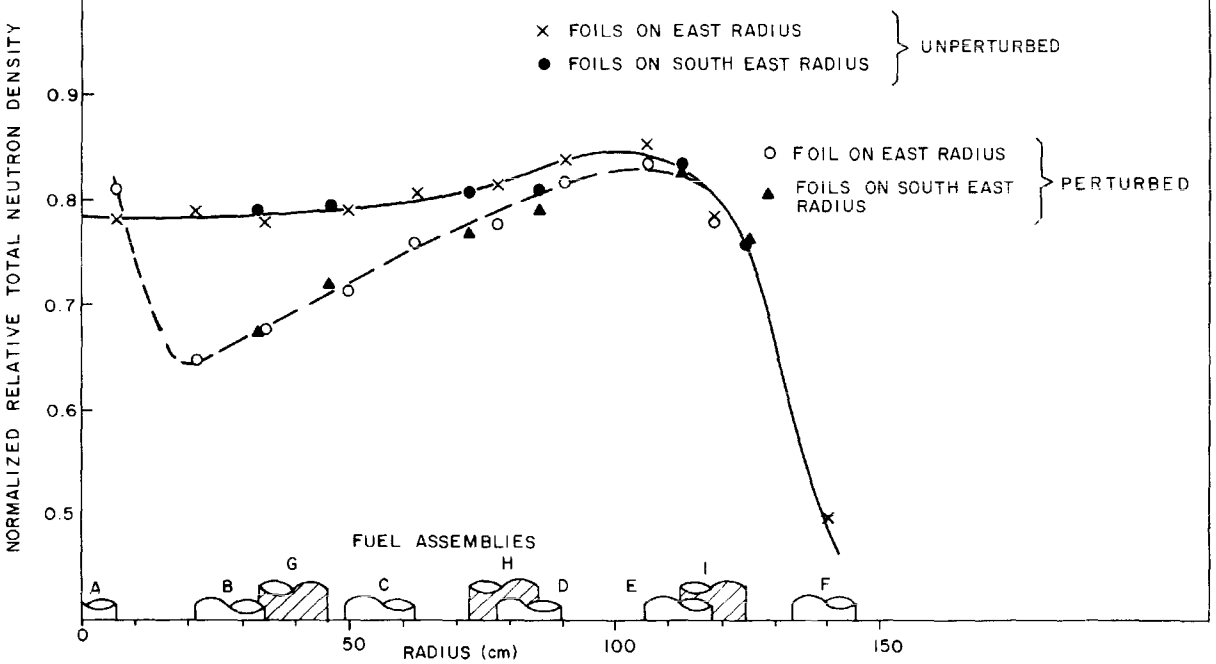

different critical heights of the reactor. This is done in terms of a flux perturbation factor F(r,z) defined by:

$$F(r,z) = \frac{\left[\frac{n(r,z)}{n(R,z)}\right]_{Perturbed}}{\left[\frac{n(r,z)}{n(R,z)}\right]_{Unperturbed}} = \frac{n'_{Perturbed}}{n'_{Unperturbed}} \quad \ldots\ldots\ldots 2)$$

where n(r,z) and n(R,z) are the relative total neutron densities at points having co-ordinates r,z, and at the same height z at radius R of thimble 'a' respectively. This thimble location was chosen as a reference position since it is a large distance away from the source of the perturbation (R = 125.9 cm) and should be unaffected by it. Figures 5, 6 and 7 illustrate the validity of this statement since the radial distributions for both the perturbed and unperturbed lattice follow the same curve at radii greater than ~ 115 cm. The results of Table 5 indicate that at radii greater than that of thimble 'a' F(r,z,) ~ 1.00. Additional justification is given by measurements of axial extrapolation length at thimble 'a' in the perturbed and unperturbed lattices (see Appendix A).

Values obtained for F(r,z) at both thimble and calandria tube locations are given in Table 5 and the mean of the values at elevations of 135 cm and 185 cm illustrated in Figure 7. All the values obtained at calandria and thimble positions can be fitted by a single curve illustrating an overall depression of the radial neutron density distribution across the pile, a minimum F(r,z) of ~ 0.82 occurring at a radius of ~ 15-20 cm from the source of the perturbation. Superimposed on this general depression, there is a peaking of F(r,z) to ~ 1.04 at the calandria tube of the water filled assembly. These effects can be qualitatively explained as follows.

TABLE 5: FLUX PERTURBATION FACTORS F(r,z)

Location	Elevation above floor of Calandria (cm) 135	185	Average	Radius cm
a	1.000	1.000	1.000	125.9
b	0.976	0.988	0.982	97.9
c	0.947	0.953	0.950	69.9
d	0.880	0.882	0.881	42.0
e	0.833	0.832	0.832	14.0
f	0.818	0.830	0.824	19.8
g	0.920	0.932	0.926	59.3
h	0.985	0.981	0.983	98.9
i	1.006	0.999	1.003	128.6
j	1.010	1.005	1.007	148.4
A(E)	1.035[b]	1.045	1.040	6.4
B(N)	0.837	0.850	0.844	28.7
B(S)	0.842	0.843	0.842	28.7
B(E)	0.868	0.867	0.867	34.3
B(W)	0.822	0.827	0.824	21.6
C(E)	0.944	0.945	0.944	62.3
C(W)	0.905	0.901	0.903	49.6
D(E)	0.973	0.967	0.970	90.3
D(W)	0.954	0.940	0.947	77.6
E(E)	0.999	0.990	0.994	118.3
E(W)	0.983	0.985	0.984	105.5
F[a]	0.996	0.991	0.994	139.9
G(NW)	0.849	0.854	0.851	45.9
G(SE)	0.905	0.900	0.902	33.2
H(NW)	0.949	0.958	0.953	85.5
H(SE)	0.977	0.968	0.971	72.8
I(NW)	0.994	0.986	0.990	125.1
I(SE)	1.008	1.000	1.004	112.3

a) Average value for two foil locations.

b) Average density of North and South foils in perturbed lattice relative to density of East foil in reference lattice.

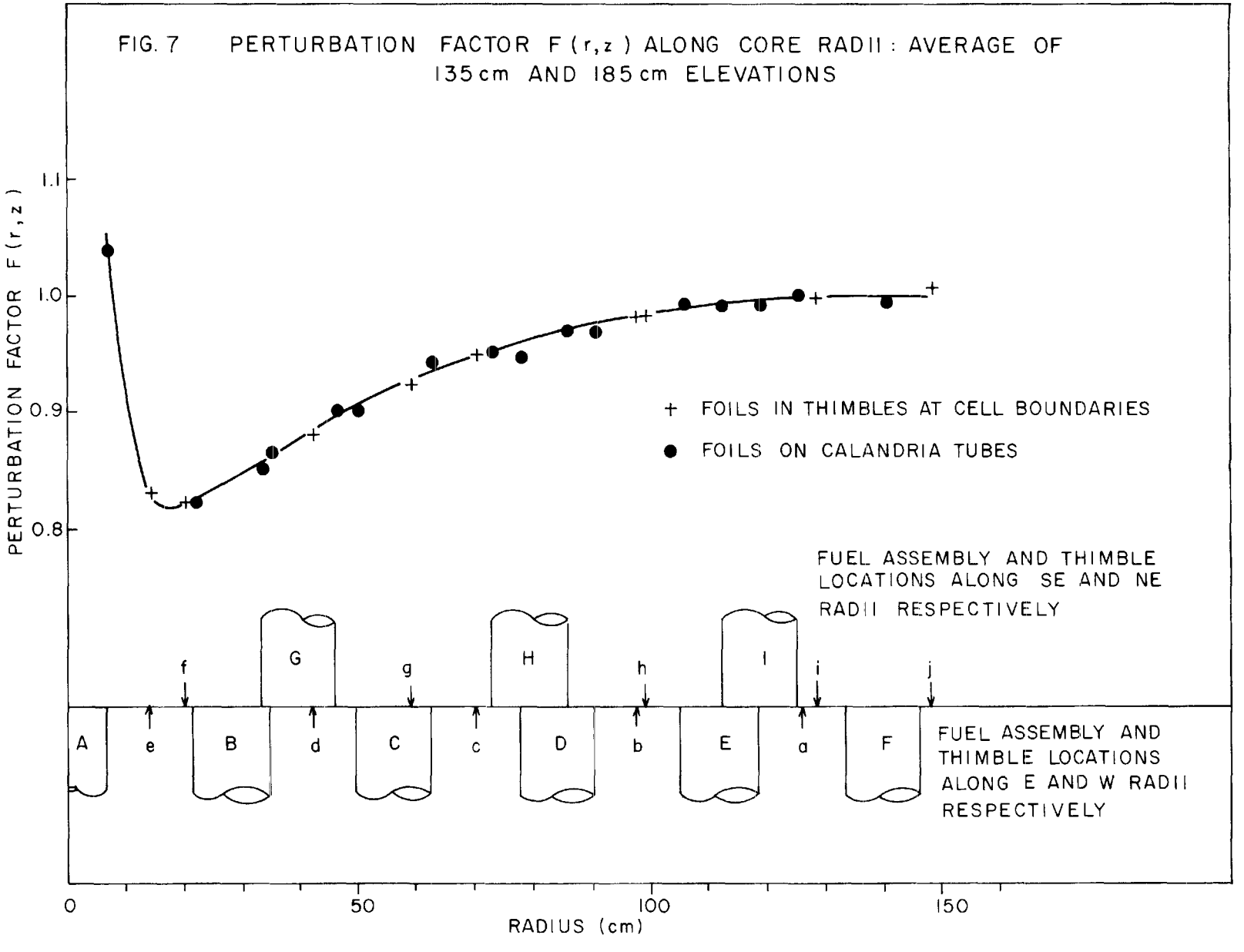

FIG. 7 PERTURBATION FACTOR F(r,z) ALONG CORE RADII : AVERAGE OF 135 cm AND 185 cm ELEVATIONS

Removal of fuel and replacement by light water decreases the total thermal neutron absorption area of the central cell by $\sim$ 80%. The loss of fuel causes a general reduction of the fast neutron density over the reactor whilst removal of absorber causes peaking of the thermal neutron density in the region of the perturbation.

Figure 7 illustrates that if the conditions of this experiment are applied to a power reactor the power generation rate in adjacent fuel assemblies will be reduced by $< \sim$ 16%.

2. Neutron Density Fine Structure and Spectrum Measurements in the Cell Containing the Light Water Filled Assembly

Table 2 lists the measured $r\sqrt{T_n/T_o}$ values at various locations in the perturbed cell. Also listed are values of

$$r\sqrt{T_n/T_o} \times n'_{\text{Perturbed}} \approx \left[n'_{\text{epi}}\right]_{\text{Perturbed}}$$

where $n'_{\text{Perturbed}}$ is defined in equation 2) and $\left[n'_{\text{epi}}\right]_{\text{Perturbed}}$ are relative values of epithermal neutron density in the perturbed lattice.

Assuming that the epithermal neutron density as determined at thimble 'e' (see Table 2), is constant over the central cell of the unperturbed lattice, then the epithermal neutron densities at the cell edge, calandria tube and centre of the central cell of the perturbed lattice are $\sim$ 50%, 30% and 10% of the unperturbed values respectively. These values reflect the effect of removing the neutron source from the central cell; the remaining epithermal density results from the incurrent from adjacent cells.

The relative activities of the manganese wires held in the lucite cruciform and on the aluminum framework were converted to relative total neutron densities using equation 1) and $r\sqrt{T_n/T_o}$ values obtained by linear interpolation from the measured values (see Table 2). This interpolation within the cell introduces negligible error since manganese has a low resonance integral and the epithermal activation was < 1% of the thermal activation at all points. Relative neutron densities on the manganese scale were converted to relative neutron densities on the copper scale using the copper-manganese normalization of Section III-4. The resulting relative total neutron densities normalized to thimble 'a' are given in Table 6 and illustrated in Figures 8 and 9.

Figure 8 illustrates the detailed relative total neutron density distribution within the light water. Relative neutron densities obtained from the manganese wires on the four arms of the cruciform show no asymmetries. The neutron density distribution within the light water filled tube is composed of two terms, a thermal neutron source term due to the good thermalizing properties of H_2O and a thermal sink term due to absorption in hydrogen. The relative magnitude of these effects will be dependent upon the ratio of fast to thermal neutron incurrents into this region. Table 2 indicates that the epithermal incurrent at the H_2O filled tube is small and Figure 8 illustrates that the dominant effect in this experiment is thermal neutron absorption. Figure 9 illustrates the neutron density distributions in two directions in the moderator surrounding the H_2O filled tube.

By numerical integration of data obtained from the eye fitted curve of Figure 8, the ratio of the average neutron density in the light water to the neutron density at the surface of the calandria tube in the perturbed cell:

TABLE 6: NORMALIZED RELATIVE TOTAL NEUTRON DENSITIES, n'(r) IN CENTRAL CELL OF PERTURBED LATTICE

Location	Radius (cm)	n'(r)	Location	Radius (cm)	n'(r)
C-S	0.50	0.5103	M-E	13.0	0.8802
C-W	0.75	0.5135	"	14.0	0.8739
C-N	1.00	0.5199	"	15.0	0.8601
C-E	1.25	0.5241	"	16.0	0.8500
C-S	1.50	0.5291	"	17.0	0.8283
C-W	1.75	0.5417	"	18.0	0.8102
C-N	2.00	0.5535	M-SE	7.0	0.8412
C-E	2.25	0.5618	"	8.0	0.8584
C-S	2.50	0.5756	"	9.0	0.8745
C-W	2.75	0.5939	"	10.0	0.8948
C-N	3.00	0.6138	"	11.0	0.8978
C-E	3.25	0.6261	"	12.0	0.9109
C-S	3.50	0.6408	"	13.0	0.9182
C-W	3.75	0.6707	"	14.0	0.9155
C-N	4.00	0.6974	"	15.0	0.9236
C-E	4.25	0.7128	"	16.0	0.9306
C-S	4.50	0.7333	"	17.0	0.9257
C-W	4.75	0.7754	"	18.0	0.9348
M-E	7.0	0.8336	"	19.0	0.9299
"	8.0	0.8514	"	20.0	0.9255
"	9.0	0.8661	"	21.0	0.9286
"	10.0	0.8743	"	22.0	0.9278
"	11.0	0.8797	"	23.0	0.9248
"	12.0	0.8796	"	24.0	0.9222

C-S, C-W, C-N, C-E refer to the South, West, North and East arms of the cruciform respectively.

M-E and M-SE refer to the East and Southeast arms of the aluminum framework respectively.

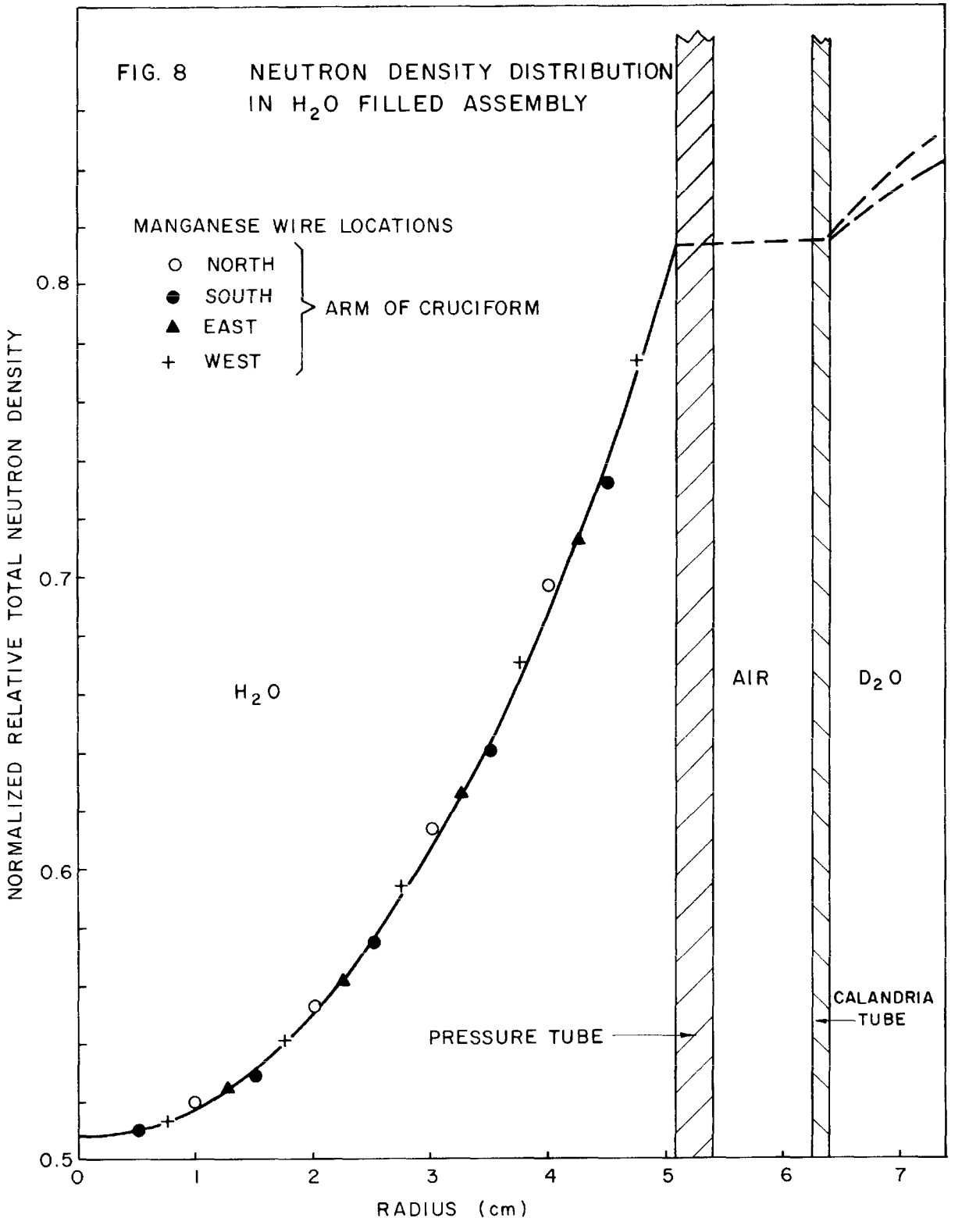
FIG. 8 NEUTRON DENSITY DISTRIBUTION IN H_2O FILLED ASSEMBLY
MANGANESE WIRE LOCATIONS
NORTH
SOUTH
EAST
WEST
ARM OF CRUCIFORM
NORMALIZED RELATIVE TOTAL NEUTRON DENSITY
0.5
0.6
0.7
0.8
0
1
2
3
4
5
6
7
RADIUS (cm)
H_2O
AIR
D_2O
PRESSURE TUBE
CALANDRIA TUBE

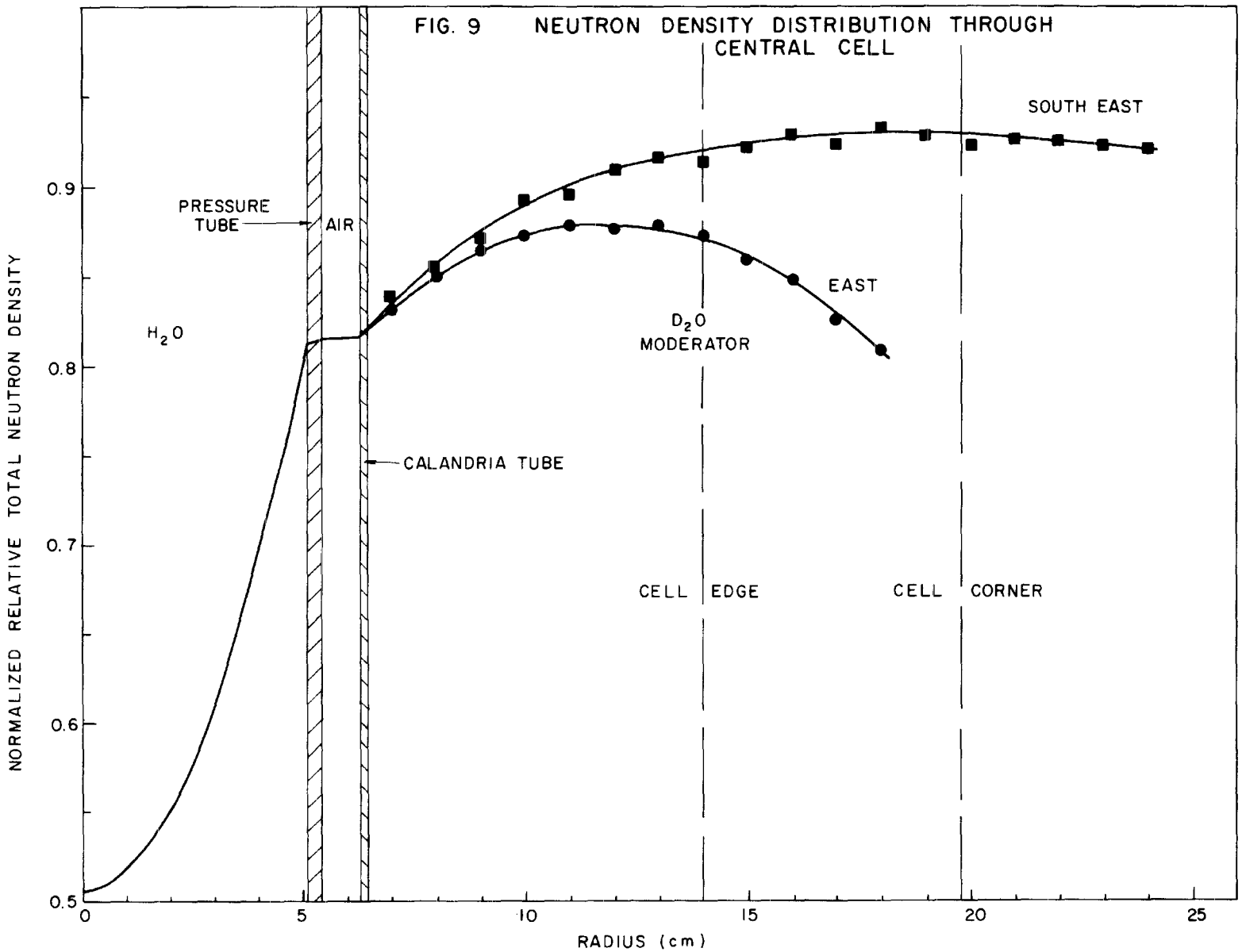
FIG. 9 NEUTRON DENSITY DISTRIBUTION THROUGH CENTRAL CELL
NORMALIZED RELATIVE TOTAL NEUTRON DENSITY
0.5
0.6
0.7
0.8
0.9
0
5
10
15
20
25
RADIUS (cm)
SOUTH EAST
EAST
PRESSURE TUBE
AIR
H_2O
D_2O MODERATOR
CALANDRIA TUBE
CELL EDGE
CELL CORNER

$$\frac{\bar{n}_{H_2O}}{\left[n_{ct.}\right]_{Pert.}} = 0.802$$

Combining this with the results of Table 5, the ratio of the average neutron density in the light water to the neutron density at the surface of the calandria tube in the unperturbed cell,

$$\frac{\bar{n}_{H_2O}}{n_{ct.}} = 0.834, \quad \text{was obtained.}$$

From previous fine structure experiments performed in an unperturbed cell[6], relative neutron densities obtained at various cell locations give the ratio of the neutron density at the surface of the calandria tube to the average neutron density in the fuel,

$$\frac{n_{ct.}}{\bar{n}_{UO_2}} = 1.82 \ ,$$

hence the ratio of the average neutron density in the light water of the perturbed cell to the average neutron density in the fuel of an unperturbed cell is

$$\frac{\bar{n}_{H_2O}}{\bar{n}_{UO_2}} = 1.52$$

Table 7 gives neutron density ratios at various locations in the region of the perturbation relative to the average value in the light water and f_{H_2O} defined as

$$f_{H_2O} = \frac{(n V \hat{\Sigma}_a)_{H_2O}}{\sum_i (n V \hat{\Sigma}_a)_i}$$

where n_i, V_i, and $\hat{\Sigma}_{ai}$ are the relative total neutron density, volume and effective absorption cross section for the i th region of the central cell of the lattice (i.e. the perturbed cell).

3. Reactivity Measurements

The reactivity effects on the central cell of the lattice due to the various perturbations, 'P', can be derived from the measured pile critical heights using the relation

$$\delta k_\infty \Big|_{cell}^{P} = C\ \Delta B_z^2 = C\ \pi^2 \left[\frac{1}{(H_c + \Delta H)^2} - \frac{1}{H_c^2} \right] \quad \ldots\ldots\ldots\ 3)$$

where H_c is the extrapolated pile height ($= H_{D_2O} + \delta_z'$) for the unperturbed system; δ_z' is a measure of the axial extrapolation length (= 21.7 cm by experiment), and ΔH is the increase in critical height required to keep the reactor critical when the perturbation is present. C is a constant of the reactor for these experiments and can be determined from the cobalt wire calibration experiment by comparing the value of $\delta k_\infty \Big|_{cell}^{Co}$ obtained from the measured critical height change, with the value calculated using the known cobalt cross section and flux depression factor, and measured cell fine structure.

Analytically the reactivity effect of the cobalt wire on

TABLE 7: FLUX ADVANTAGE FACTORS AND f_{H_2O} IN PERTURBED CELL

$\frac{\bar{n}_{H_2O}}{\bar{n}_{UO_2}}$	$\frac{\bar{n}_{pt}}{\bar{n}_{H_2O}}$	$\frac{\bar{n}_{ct}}{\bar{n}_{H_2O}}$	$\frac{\bar{n}_{a.}}{\bar{n}_{H_2O}}$	$\frac{\bar{n}_{mod.}}{\bar{n}_{H_2O}}$	f_{H_2O}
1.516	1.244	1.247	1.246	1.358	0.826

H_2O, pt, ct, a., and mod., refer to average values in the light water, pressure tube, calandria tube, air gap and moderator of the perturbed cell.

TABLE 8: LATTICE REACTIVITY DATA

Experiment	H_c cm	ΔH cm	ΔB_z^2 cm^{-2}	$\delta k_\infty \Big\|_{cell}^{P}$ mk
H_2O Filled Assembly	266.108	+11.527	-0.1134×10^{-4}	-411
Air Filled Assembly	266.061	+ 3.468	-0.0357×10^{-4}	-129
D_2O Filled Assembly	265.981	+ 3.075	-0.0317×10^{-4}	-115
Cobalt Wire in Central Cell	265.969	+ 0.740	-0.0773×10^{-5}	- 28

the central cell is given by

$$\delta k_\infty \Big|_{\text{cell}}^{\text{Co}} = -(d\hat{\Sigma}V)_{\text{Co}} \Big/ \frac{(\hat{\Sigma}V)_{UO_2}}{f(1 + L_s^2 B^2)} \quad \ldots\ldots\ldots 4)$$

where $(d\hat{\Sigma}V)_{\text{Co}}$ is the increase in the absorption in the central cell due to the cobalt wire $\left[(\hat{\Sigma}V)_{\text{Co}} = 0.1053 \text{ cm}^2/\text{cm length}\right]$, B^2 is the measured buckling of the 28-rod cell (see appendix A) and

f, $\hat{\Sigma}_{UO_2}$ and L_s^2 have their usual meanings (values of f and L_s^2 were obtained using the LATREP code[9]).

Using equation 4) and appropriate values for the parameters gives

$$\delta k_\infty \Big|_{\text{cell}}^{\text{Co}} = -28.0 \text{ milli-k}$$

and hence using equation 3) and the measured change in axial buckling for the cobalt wire

$$C = \frac{\delta k_\infty \Big|_{\text{cell}}^{\text{Co}}}{\Delta B^2_{\text{Co}}} = \frac{-28.0}{-7.73 \times 10^{-7}} = 3.62 \times 10^7 \text{ milli-k/cm}^{-2}$$

Since C is a constant, equation 3) becomes

$$\delta k_\infty \Big|_{\text{cell}}^{\text{P}} = 3.62 \times 10^7 \ \Delta B_z^2 \quad \ldots\ldots\ldots 5)$$

Table 8 lists the extrapolated critical heights of the unperturbed pile H_c, the increase in critical height due to the

perturbation ΔH , the change in axial buckling ΔB_z^2 and the corresponding change in reactivity of the central cell $\delta k_\infty \Big|_{cell}^{P}$ obtained using equation 5). All values are corrected to a temperature of 22.35°C at a D_2O purity of 99.70 a/o D_2O.

CONCLUSIONS

Experiments have been performed using a simulated CANDU-BLW core in ZED-2 to investigate the reactivity effect and the perturbing effect on the surrounding lattice when the fuel in the central channel of the lattice is replaced by light water, this procedure approximating two of the stages in the refuelling sequence of the proposed BLW power reactor.

Removal of the fuel reduces the neutron source strength at the perturbation and depresses the neutron density distribution in the region surrounding the perturbation. Replacement of the fuel by light water results in a net reduction in the absorption of the perturbed cell, this results in a local peaking of the neutron density at the perturbation. The net effect is a reduction in neutron density at all fuel sites surrounding the perturbation, a maximum perturbation of $\sim$ -18% occurring at a distance $\sim$ 15-20 cm away from the centre of the perturbation. The maximum effect on the neutron density in surrounding fuel assemblies is a depression $\sim$ 16% at the assembly closest to the perturbation.

Although the results obtained from these experiments are not directly applicable to the proposed power reactor, because of differences in the lattice properties, they do indicate the relative magnitudes of the changes in source strength, absorption and slowing down caused by the perturbation and serve as a normalization for computer codes.

Results of reactivity measurements associated with the 'refuelling' are expressed relative to the reactivity effect of a known absorber in the lattice. Application of these ratios to the prototype reactor must take into account the different cell compositions and detailed neutron density distributions.

Due to the magnitude and 'multi-energy group' nature of the perturbations no attempt is made in this report to compare experiment with theory.

ACKNOWLEDGEMENTS

The authors wish to thank the many people involved in performing the experiments and the production of this report, in particular to P.D.J. Ferrigan, E. Pleau and D.J. Roberts who arranged the lattice in the reactor, J.T.R. Young who was responsible for the counting of the foils and wires, Mrs. A. Brum and Miss D. Graham who helped analyse the data, the typists of the Stenographic Services who typed the manuscript, R.E. Green for advice on performing the experiments and the writing of the manuscript and C.H. Millar for criticism of the manuscript.

REFERENCES

1. ZED-2, AECL-2132 (1964)

2. G.A. PON, CANDU-BLW-250 Progress Report, AECL-2554 (1966)

3. D. PRIMEAU, Private Communication (1966).

4. D.W. HONE et al. Natural Uranium Heavy Water Lattices, Experiment and Theory, AECL-622 (1958).

5. R.E. GREEN et al. Lattice Studies at Chalk River and Their Interpretation, AECL-2025 (1964).

6. P. FRENCH, Private Communication (1966)

7. C.B. BIGHAM et al. Experimental Effective Fission Cross Sections and Neutron Spectra in a Uranium Fuel Rod, AECL-1186 (1961).

8. C.H. WESTCOTT, Effective Cross Section Values for Well Moderated Thermal Reactor Spectra, AECL-1101 (1964).

9. I.H. GIBSON, The Physics of LATREP, AECL-2548 (1966).

10. C.W. COLPITTS et al. Progress Report PR-RRD-47 Sect. 4.3.1.2 (1966)

11. R.E. GREEN et al. Progress Report PR-RRD-48 Sect. 4.3.1.4 (1966)

APPENDIX A

Axial and Radial Bucklings for the BLW(AS) Core

As mentioned in Section III-1, copper foil activity data obtained from thimbles 'e', 'a' and 'j' in the unperturbed lattice at core radii of 14.0 cm, 125.9 cm and 148.4 cm respectively was used to determine axial bucklings.

Least squares cosine fits to copper foil activities, using data away from bundle ends and between elevations of 45 cm and 205 cm (i.e. well away from core boundaries), were made using the expression

$$A(z) = A(z_o) \cos \alpha'(z-z_o),$$

z_o is the point of maximum flux and

α'^2 the axial buckling of the core containing thimbles and foils.

Table A1 lists the values obtained, δ_z' is a measure of the total axial extrapolation length and is obtained using

$$\delta_z' = \frac{\pi}{\alpha'} - H'_{D_2O},$$

where H'_{D_2O} is the heavy water height for the core containing thimbles and foils.

Values of axial buckling are determined by the properties of the cell and the effects of adjacent boundaries. The buckling measured at thimble 'e', well away from boundaries, is a measure of the axial buckling in the simulated BLW region whilst values

TABLE A1: SUMMARY OF LEAST SQUARES FITS

Region of Fit	Axial or Horizontal and elevation (cm)	No. of Points Fitted	ν m-1	α' m-1	z_o cm	δ_z' cm
Thimble e	A	17		1.185	117.6	20.7±2.6
Thimble a	A	17		1.182	117.8	21.3±2.7
Thimble j	A	17		1.167	117.2	24.7±4.0
Thimble a perturbed	A	18		1.129	123.1	22.6±2.6
Thimbles:West	H(135)	3	0.490			
"	H(185)	3	0.504			
Thimbles:Northeast	H(135)	3	0.436			
"	H(185)	3	0.530			
Calandria:East	H(135)	7	0.490			
"	H(185)	7	0.514			
Calandria:East + Southeast	H(135)	10	0.490			
"	H(185)	10	0.564			

of buckling obtained at thimbles 'a' and 'j' are affected by the graphite reflector which effectively reduces the axial leakage in that region.

The axial buckling of the BLW region of the core with no thimbles or foils present, α^2_{BLW}, was determined using the δ_z' of Table A1, the bare pile (i.e. no thimbles or foils) critical height, H_{D_2O} (= 243.995 at 22.97°C, 99.70a/o D_2O) and the expression

$$\alpha^2_{BLW} = \frac{\pi^2}{(H_{D_2O} + \delta_z')^2}$$

giving

$$\alpha^2_{BLW} = 1.409 \pm 0.028 m^{-2} \quad (22.97°C, 99.70a/o)$$

Figures 5 and 6 illustrate the radial neutron density distributions in the unperturbed core. Because of the non-uniformity of the core this distribution is complex and in the BLW region follows an I_o distribution. Radial least squares fits were made to the expression

$$A(r) = A(r_o) I_o(\nu r)$$

of the neutron density data of Table 3 using points in the BLW region further than $\sqrt{2}$ x (BLW lattice pitch) away from 7-rod UO_2 or ZEEP fuel assemblies.

Results of these fits listed in Table A1 give a mean value of radial buckling (ν^2) in the BLW region of

$$\nu^2_{BLW} = \underline{0.252 \pm 0.035\ m^{-2}}\ (22.44^\circ C,\ 99.70\ a/o)$$

Combining the axial and radial results and assuming ν^2 independent of temperature, the buckling of the BLW region of the core

$$B^2_{BLW} = \left(\alpha^2_{BLW} - \nu^2_{BLW}\right)$$

$$= \underline{1.157 \pm 0.045\ m^{-2}}\ (22.97^\circ C,\ 99.70\ a/o\ D_2O)$$

This value is in good agreement with the previously measured buckling for this lattice[10][11].

Table A1 also lists results obtained from a cosine fit to the axial copper foil activity distribution in thimble 'a' of the perturbed lattice (i.e. when the fuel in assembly A is replaced by light water). The δ'_z values obtained at thimble 'a' in both the perturbed and unperturbed lattice are in good agreement within the limits of error. This result supports the assumption of Section IV-1 that the effect of the perturbation at thimble 'a' is negligible.